

Stem respiration in tropical forests along an elevation gradient in the Amazon and Andes

AMANDA L. ROBERTSON*, YADVINDER MALHI†, FILIO FARFAN-AMEZQUITA‡, LUIZ EDUARDO O. C. ARAGÃO‡, JAVIER EDUARDO SILVA ESPEJO‡ and MATTHEW A. ROBERTSON§

*Biology and Wildlife Department, University of Alaska Fairbanks, 211 Irving I, Fairbanks, AK 99775, USA, †Environmental Change Institute, School of Geography and the Environment, Oxford University, South Parks Road, Oxford OX1 3QY, U.K., ‡Universidad San Antonio Abad, Cusco, Peru, §Forest Sciences Department, University of Alaska Fairbanks, 335 O'Neill, Fairbanks, AK 99775, USA

Abstract

Autotrophic respiration involves the use of fixed carbon by plants for their own metabolism, resulting in the release of carbon dioxide as a by-product. Little is known of how autotrophic respiration components vary across environmental gradients, particularly in tropical ecosystems. Here, we present stem CO₂ efflux data measured across an elevation transect spanning ca. 2800 m in the Peruvian Amazon and Andes. Forest plots from five elevations were studied: 194, 210, 1000, 1500, and 3025 m asl. Stem CO₂ efflux (R_s) values from each plot were extrapolated to the 1-ha plot level. Mean R_s per unit stem surface area declined significantly with elevation, from 1.14 ± 0.12 at 210 m elevation to $0.62 \pm 0.09 \mu\text{mol C m}^{-2} \text{s}^{-1}$ at 3025 m elevation. When adjusted for changing forest structure with elevation, this is equivalent to $6.45 \pm 1.12 \text{ Mg C ha}^{-1} \text{ yr}^{-1}$ at 210 m elevation to $2.94 \pm 0.19 \text{ Mg C ha}^{-1} \text{ yr}^{-1}$ at 3025 m elevation. We attempted to partition stem respiration into growth and maintenance respiration components for each site. Both growth and maintenance respiration rates per unit stem showed similar, moderately significant absolute declines with elevation, but the proportional decline in growth respiration rates was much greater. Stem area index (SAI) showed little trend along the transect, with declining tree stature at higher elevations being offset by an increased number of small trees. This trend in SAI is sensitive to changes in forest stature or size structure. In the context of rapid regional warming over the 21st century, such indirect, ecosystem-level temperature responses are likely to be as important as the direct effects of temperature on maintenance respiration rates.

Keywords: altitudinal gradient, Amazon, autotrophic respiration, carbon cycle, CO₂ efflux, stem area index, tropical montane forest

Received 4 December 2009 and accepted 28 June 2010

Introduction

Tropical forests play a major role in the global carbon (C) cycle (Malhi & Grace, 2000). The C cycle of forest ecosystems includes the uptake of CO₂ during photosynthesis and the release of C from autotrophic respiration for growth and the maintenance of stems, roots, and leaves. The proportion of C allocated to growth or released as a by-product of respiration should vary between different soil types, climates, and growth strategies (Luyssaert *et al.*, 2007).

There is mounting concern about changing carbon balances in tropical forests (e.g. shifting from over-all carbon sinks to carbon sources) in the face of global climate change (Saxe *et al.*, 2001). Warmer and possibly drier conditions, such as those projected for the

Amazon Basin, have been associated with potential large-scale increases in C effluxes in tropical forests (Meir *et al.*, 2008; Phillips *et al.*, 2009). In order to understand how forest systems may respond under predicted climate regimes, it is first necessary to establish baseline data for broad-scale (i.e. landscape-level) extrapolations. In Amazonia, some work towards this effort has been undertaken, linking bottom-up with top-down approaches to the quantification of C dynamics, and scaling across heterogeneous landscapes (Chambers *et al.*, 2004; Luyssaert *et al.*, 2007; Aragão *et al.*, 2009; Malhi *et al.*, 2009). To date very few studies have taken a similar approach to quantifying the C budgets of tropical montane forests; the work presented here is part of a systematic effort to quantify carbon dynamics along an elevation transect in the Andes.

Autotrophic respiration (R_a) makes up a large portion of the C that is returned to the atmosphere from forests. R_a has been estimated as 40–70% of C assimilated via

Correspondence: Amanda L. Robertson, tel. +1 907 474 6232, fax +1 907 474 6716, e-mail: arobertson2@alaska.edu

photosynthesis in temperate forest ecosystems (Ryan *et al.*, 1995; reviewed by Saxe *et al.*, 2001). Chambers *et al.* (2004) estimated that 70% of assimilated C is released as autotrophic respiration in a Central Amazon forest. Stem respiration is the efflux of CO₂ from the metabolic activity of woody cells associated with maintenance and growth processes, and is a substantial contributor to total autotrophic respiration (Malhi *et al.*, 2009). Stem woody CO₂ efflux is largely a measure of stem respiration, the *in situ* autotrophic respiration of the biologically active outer layer of the stem, although an unquantified component of the CO₂ efflux may be from CO₂ dissolved in the transpiration stream, and ultimately coming from either from root metabolism (Teskey & McGuire, 2002; Aubrey & Teskey, 2009) or soil heterotrophic respiration (R_h) transported from the roots via the xylem (Bowman *et al.*, 2005; Meir *et al.*, 2008). Our implicit assumption in this paper is that stem woody CO₂ efflux is largely a measure of stem respiration and hence is abbreviated R_s , although we recognize the potential presence of a bark-diffused xylem-transported CO₂ component.

Compared with carbon fixation (e.g. photosynthesis), autotrophic and heterotrophic respiration are much less studied and harder to quantify (Harris *et al.*, 2008). Differences in soil type/nutrient content, forest type and land-cover history are expected to result in different balances of R_a and R_h (Trumbore, 2006). Few studies have attempted to quantify how autotrophic respiration varies across the landscape. Plot-level, or ground-up studies are crucial for extrapolating respiratory components of forest ecosystems and to validate eddy-covariance flux or remote methods.

Here, we exploit a tropical elevation gradient to explore how woody-tissue CO₂ efflux rates respond to a gradient in elevation, which we take as fundamentally being a gradient in long-term mean temperature. Across a wet tropical elevation transect there is little seasonal variation in temperature, and no dormant season that confounds interpretation of such analyses along mid-high latitude elevation gradients. We hypothesize that stem CO₂ efflux per unit stem and ground area will decline with increasing elevation due to decreasing temperature and changing tree stature.

The objectives of this study are to (i) compare R_s along an elevation transect in the Andes, (ii) explore how stem area indices vary along the elevation gradient, (iii) attempt to separate R_s into maintenance and growth components, (iv) scale R_s to 1 ha based on a subset of measured trees in the plot, and (v) explore the extent to which changes in forest structure and metabolism cause changes in ecosystem woody respiration. This elevation transect presents a natural laboratory in which to address how forest C budgets change with altitude, and by

inference, an opportunity to explore the potential influence of temperature on ecosystem function.

Materials and methods

Study sites

The elevation transect is established in southern Peru (Fig. 1) and spans approximately 2800 vertical metres. The foci of this study are five study sites including five 1-ha long-term forest monitoring plots at each site and four smaller plots (ranging from 0.04 to 0.14 ha at four of the five study sites) located from 194 m elevation to 3025 m (Table 1). At least one study site is included from each of the following forest categories: upper-montane cloud forest (2200–3400 m asl), lower-montane cloud forest (1500–2200 m asl), pre-montane forest (800–1500 m asl), and lowland rainforest (<800 m asl). The 1-ha 3025 m plot is actually 1.2 ha in area due to the sloped terrain (projected area is 1 ha); plot area was corrected to 1 ha in all analyses relating to stem area index. This study is a component of a suite of projects attempting to quantify plot-level aspects of tropical montane forest carbon cycling within the Andes Biodiversity and Ecosystems Research Group (ABERG).

Weather stations were in place in all Andean plots and close to the lowland plots. The air temperature lapse rate is 4.94 °C km⁻¹ (Girardin *et al.*, in press). There is little evidence of seasonality in air temperature although but a defined dry season between June and September (Girardin *et al.*, in press). Soil water content also does not vary substantially with elevation (C. A. J. Girardin, L. E. O. C. Aragão, Y. Malhi, W. Huaraca Huasco, D. Metcalfe, L. Durand, M. Mamani, J. Silva-Espejo, unpublished results), and in particular showed almost no seasonal variation above 1000 m elevation, presumably because cloud immersion (cloud deposition and reduced transpiration) in the montane forests prevents the onset of water stress. There are no significant differences in soil phosphorous (P) between elevations and soil N initially declines with elevation but there is no difference between the highest and lowest elevation plots (Table 1); however, foliar N:P data suggest increasing P limitation and decreasing N limitation with increasing elevation (J.A.B. Fisher, unpublished analysis). There are no clear trends in basal area or stem density with elevation (Table 1); declining aboveground biomass with increasing elevation is mainly explained by decreasing canopy height (Girardin *et al.*, in press).

At the lowland study location, long-term forest plots have been extensively studied as part of the Amazon Forest Inventory Network (RAINFOR) in the Tambopata Biological Reserve, Madre de Dios Region, Peru (Fig. 1). All trees and lianas ≥ 10 cm diameter at breast height (dbh, measured 1.3 m above soil level) have been taxonomically surveyed. We measured R_s within two 1-ha plots, TAM-06 (194 m asl) and TAM-05 (210 m asl); plot characteristics can be found in Table 1. At both sites, the average canopy height for both Tambopata plots is approximately 35 m (Aragão *et al.*, 2009), and average annual length of dry season (<100 mm monthly precipitation) is 3.5 months (Malhi *et al.*, 2004). In addition to the 1-ha plots, one 0.1-ha (10 × 100 m) permanent tree plot was

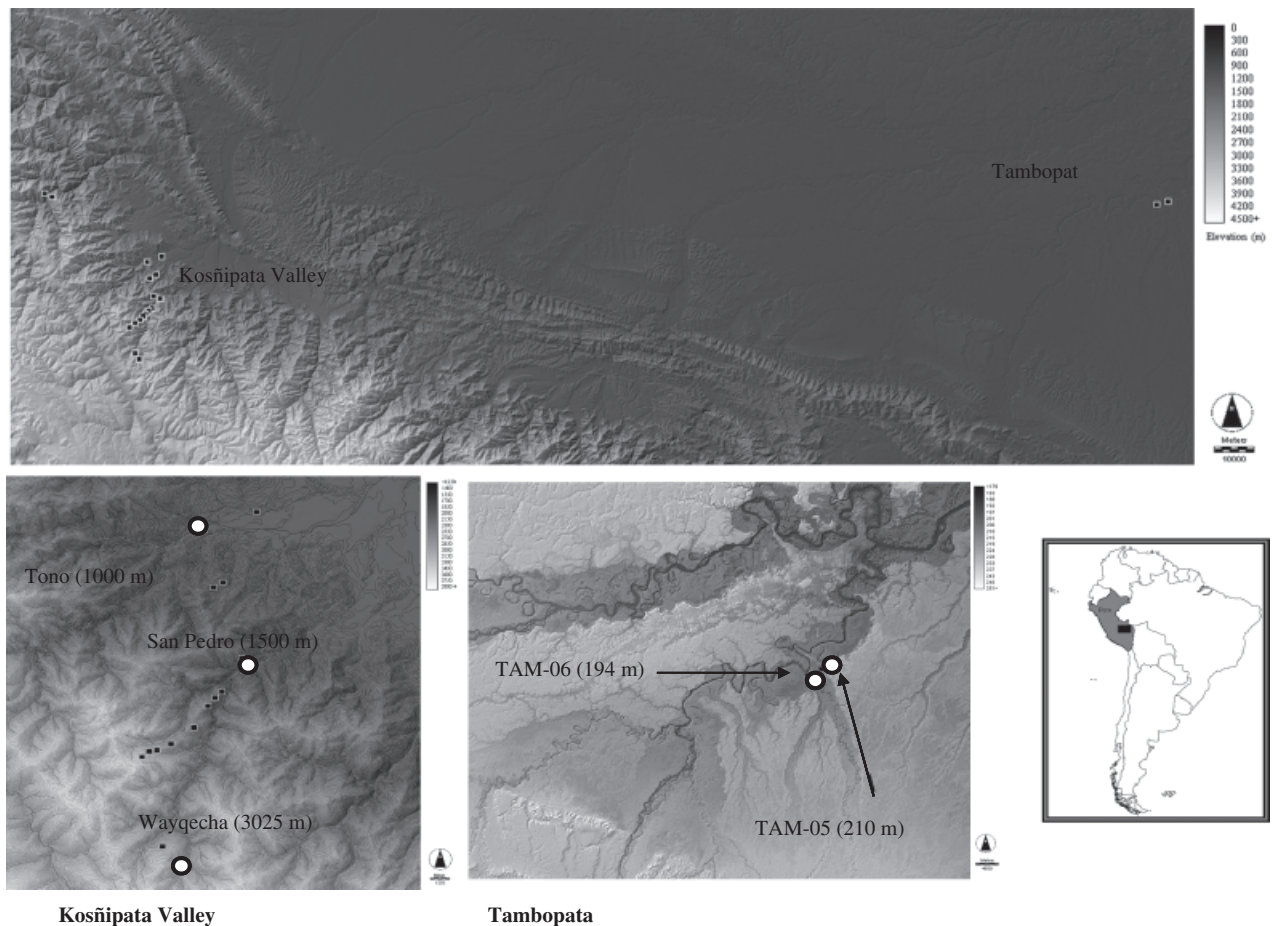


Fig. 1 Location and elevation of study sites (circled) in the Peruvian Andes in context of South America (lower right panel). The top panel shows the entire elevation transect from 3025 to 194 m elevation on the Eastern flank of the Peruvian Andes.

included next to both TAM-05 and TAM-06, here referred to as TAM-05_{small} and TAM-06_{small}. In these small plots all trees and lianas ≥ 2 cm dbh have been measured and catalogued, but are yet to be taxonomically identified; the purpose of measuring stem respiration on the smaller tree component is to quantify the contribution of CO₂ efflux from the forest understory (trees and lianas under 10 cm dbh).

The montane part of the transect is located in the Manu National Park, on the eastern slope of the Peruvian Andes, in the Kosñipata Valley (Province of Paucartambo, Department of Cusco, Peru; Fig. 1). One-hectare permanent tree plots were established between 2003 and 2005 by ABERG and all trees and lianas ≥ 10 cm dbh have been catalogued. The three Andean plots, Tono (1000 m asl), San Pedro (1500 m asl) and Wayqecha (3025 m asl) in addition to the 1-ha Tambopata plots (194 and 210 m asl) were used for the elevation comparison of stem respiration. The Andean plots are referred to by elevation only from this point forward. Additional small-tree plots (all trees dbh ≥ 2 cm dbh) were nested within the 1500 m plot (0.04 ha, consisting of one 20 \times 20 m plot; 1500_{small}) and within the 3025 m plot (0.14 ha, consisting of one 20 \times 20 m and four 16 \times 16 m plots; 3250_{small}). These small plots are used here to

characterize the forest understory, however, no R_s measurements were taken within these plots as they were established after this study was conducted.

Sample design

Within each of the five 1-ha plots included in this study, 50 trees ≥ 10 cm dbh were randomly chosen for measurement, stratified by relative growth rate (lowland plots) or dbh (Andes plots). At the time trees were chosen for measurement, growth-rate data were not available for the (then single census) montane sites and thus sample stratification by growth rate was not possible. Growth data were collected concurrently with this study. Tree diameters and growth rates were determined via recensused dbh data and tri-monthly dendrometer band measurements. Ten trees were randomly chosen from each of five annual growth-rate classes [0 cm yr⁻¹ (no growth), 0.01–0.19, 0.20–0.49, 0.5–0.69, and ≥ 0.70 cm yr⁻¹] or diameter classes [10.0–12.9, 13.0–15.9, 16.0–20.9, 21.0–25.9, ≥ 26.0 cm].

At 194 m, 32 species were selected for measurement including nine individuals from the dominant palm species, *Iriartea*

Table 1 Site characteristics for the plots included in the elevation transect, including mean annual precipitation (MAP), mean annual air temperature (MAT), and mean measured stem temperature (MST) for the measurement interval in May 2007

Plot ID	Elevation (m)	Plot area (ha)	Stem CO ₂ efflux measured	MAP (mm)	MAT (°C)	MMT (°C)	Basal area (m ² ha ⁻¹)	Stem density (stems ha ⁻¹)	Soil type
TAM-06	194	1.0	Yes	2730	26.4	26.4	35.3	665	Holocene alluvial terrace
TAM-06 _{small}	194	0.1	Yes	2730	26.4	26.4	12.3	1110	Holocene alluvial terrace
TAM-05	210	1.0	Yes	2730	26.4	24.0	26.4	535	Pleistocene alluvial terrace
TAM-05 _{small}	210	0.1	Yes	2730	26.4	24.0	12.3	1080	Pleistocene alluvial terrace
Tono	1000	1.0	Yes	3087	20.7	21.8	29.4	412	Alluvial terrace
San Pedro	1500	1.0	Yes	2631	18.8	17.8	35.4	687	Paleozoic shales-slates
1500 _{small}	1500	0.04	No	2631	18.8	17.8	4.5	1800	Paleozoic shales-slates
Wayqecha	3025	1.0	Yes	1706	12.5	12.2	19.3	1060	Paleozoic shales-slates
3025 _{small}	3025	0.14	No	1706	12.5	12.2	3.4	1225	Paleozoic shales-slates

Soil/climate data from C. A. J. Girardin, L. E. O. C. Aragão, Y. Malhi, W. Huaraca Huasco, D. Metcalfe, L. Durand, M. Mamani, J. Silva-Espejo (unpublished results).

deltoidea (Palmaceae). Thirty-five tree species were sampled from 210 m; three species were palms representing four individuals. Only two sampled species were present at more than one elevation: *Iriartea deltoidea* was sampled at both 194 and 210 m, and *Virola elongata* (Myristicaceae) was sampled from 194 and 1000 m. In each of TAM-05_{small} and TAM-06_{small}, 25 additional trees and lianas between 0.2 and 10 cm dbh were randomly chosen for measurement. Measurements in TAM-05_{small} included two lianas whereas lianas represented 13 of the 25 individuals in TAM-06_{small}. The trees selected for measurement at 1000 m included 27 species (not including 13 unidentified morphotypes), individuals from 2000 m comprised 30 species (not including 15 unidentified individuals), and measured trees within the 3000 m plot represented 25 species with 19 individuals representing the dominant taxon, *Weinmannia crassifolia* (Cunoniaceae).

CO₂ efflux measurements

Woody-tissue CO₂ efflux was quantified using a field-portable, closed dynamic chamber system incorporating an infra-red gas analyzer and datalogger (LI-820, LI-1400, LiCor, Lincoln, NE, USA). A polyvinyl chloride (PVC) semi-cylindrical chamber was secured to the base of each tree/liana at 1.3 m above ground (or above buttresses) using nylon straps (chambers ranged in volume from 245 to 784 mL; chambers were chosen to best fit each individual bole). Closed-cell foam and silicon were used to create a secure seal and breathing tests were conducted near each tree to insure a proper seal. Any mosses or epiphytes were removed using a soft brush before securing the chambers. The concentration of CO₂ within the chambers was measured for 2 min per tree. The field equipment and methods were adapted from Chambers *et al.* (2004). Measurements at all sites were taken during the day in the early dry season in May, 2007.

Plots of CO₂ concentration against time were checked for linearity for each measurement. Plots were discarded if the coefficient of determination, r^2 , for a linear regression of CO₂

concentration against time was ≤ 0.80 and all but four samples ($N = 242$) had $r^2 \geq 0.90$. Stem CO₂ efflux per unit stem surface area over time was calculated using the following equation (PP-Systems, 2002):

$$R_s = \left(\frac{S \left(\frac{P}{101.3} \right) \left(\frac{273.5}{T+273.15} \right) M \left(\frac{V}{A} \right)}{1000} \right) \times 3600 \times 6.132, \quad (1)$$

where R_s is the woody tissue CO₂ efflux per unit stem surface area ($\mu\text{mol C m}^{-2} \text{s}^{-1}$); S is the slope of the change in CO₂ concentration over time in the chamber (ppm s^{-1}); P is the pressure (kPa); T is the ambient temperature ($^{\circ}\text{C}$); M is the volume of one mole of CO₂ ($22.41 \times 10^{-4} \text{ m}^3$ at STP); V is the total volume of the chamber (m^3); A is the stem surface area covered by the chamber (m^2); the last two multiplication factors convert units to $\mu\text{mol C m}^{-2} \text{s}^{-1}$. $1 \mu\text{mol C m}^{-2} \text{s}^{-1}$ ground area is equivalent to $3.788 \text{ Mg C ha}^{-1} \text{ yr}^{-1}$. Herein values given in units of $\mu\text{mol C m}^{-2} \text{s}^{-1}$ relate to CO₂ efflux per unit stem surface area whereas $\text{Mg C ha}^{-1} \text{ yr}^{-1}$ relate to CO₂ efflux scaled to the 1-ha plot level.

Scaling stem CO₂ efflux to plot level

A challenge to 'ground-up' methods is the extrapolation from a subset of measurements to the forest level. Approaches to scaling woody CO₂ efflux have included measuring respiratory fluxes per unit live-cell (sapwood) volume scaling by estimating total-tree sapwood volume (Ryan, 1990), modelling CO₂ efflux by temperature (Hansen *et al.*, 1994), cell nitrogen content (Reich *et al.*, 2008), or bole surface area (Meir & Grace, 2002). Here, we scale to the forest level by estimating the surface area of the entire tree, or the stem area index (SAI – the surface woody area per unit ground area) for each tree in the plot (Chambers *et al.*, 2004). Large branches are implicitly included in the SAI calculations (see methods of Chambers *et al.*, 2004). This method is comparable to using leaf area index (LAI) to scale leaf respiration measurements.

Chambers *et al.* (2004) explored the relationship between the surface area of trees to dbh for broad-leaved trees ($N = 5283$) in

lowland Amazonian forests near Manaus, Brazil. We adopted their equation to calculate SAI for broad-leaf trees based on dbh measurements. SAI_{plot} is the summation of all bark surface areas (all trees in the plot) divided by the plot area:

$$SAI_{\text{plot}} = \frac{1}{A_g} \sum_{i=1}^n -0.015 - 0.686 \log(D) + 2.208 \times \log(D)^2 - 0.627 \log(D)^3, \quad (2)$$

where SAI_{plot} is the plot stem area index; D is the dbh for each tree (cm); A_g is the plot ground area (m^2). Note that Eqn (2) uses tree-allometry data specific to Central Amazon lowland forests.

We calculated the SAI of palms in a different manner, by calculating the surface area of a cylinder, as the boles of palms do not taper like broad-leaf trees and branches make little contribution to the total bark surface area. Additionally, the height of palms was adjusted to be 60% of that of broad-leaf trees of similar diameter (Frangi & Lugo, 1985). Equation (2) was not adjusted for lianas due to the low numbers of lianas in our datasets; in the five 1-ha plots, only individuals ≥ 10 cm dbh were included and few lianas enter this category.

SAI was also estimated for the small-diameter plots and scaled to 1 ha. We refer to SAI_{total} as the summation of SAI_{plot} with the estimated SAI for the understory at that elevation. As there is no small-diameter plot at 1000 m, the understory SAI for that elevation was estimated by assuming that the proportion of SAI in small trees was equal to average of this proportion in the plots at 194, 210 and 1500 m. For the purposes of error propagation, uncertainty for SAI measurements was assigned an estimated value of 10%. There is inherent error in the SAI equation as well as in the dbh measurements. Across the heterogeneous variety of the Amazon basin, SAI is calculated between 1.5 and 2.0 (unpublished data; Chambers *et al.*, 2004); given that vastly different forest structures result in a similar SAI value, an error estimate of 10% can be considered reasonable.

In the Andean plots, we adjusted the SAI calculations for canopy height. Average canopy height in forests near Manaus, where the SAI equation was derived, is 35 m (Chambers *et al.*, 2009), similar to mean canopy height for the Tambopata lowland forest. Trees in the montane forests tend not to grow as tall as lowland trees with the same dbh. We used the plot-specific equations given in Table 2 to estimate tree heights at 1000, 1500, and 3025 m (J.A.B. Fisher, unpublished analysis). SAI for each tree was multiplied by the height correction factor which was calculated as the average ratio of predicted tree

height per given dbh in the Andes plots to trees with the same dbh in the Tambopata plots (Table 2). For the same dbh, trees tend to be 39% shorter in the upper-montane cloud forest plot (3025 m), 28% shorter in the lower-montane cloud forest plot (1500 m), and 14% shorter in the pre-montane forest plot (1000 m), compared with the lowland forest at Tambopata (Table 2).

Analyses

Within-plot comparisons of R_s included looking for differences in CO_2 efflux between different functional types (e.g. palms, hardwoods, lianas) and dominant genera (e.g. *Weinmania* in high-elevation plots) as such differences have been observed in other tropical forests (Cavaleri *et al.*, 2006, 2008). This study was not initially designed to address these questions and thus only in TAM-06 was palm sample size high enough for comparison with broadleaf trees using a two-sample *t*-test assuming unequal variances. R_s measurements for lianas were singled out in TAM-06_{small}. *Weinmania* was compared with other genera within the 3025 m plot also using a *t*-test assuming unequal variances. Statistical differences in respiration rate between functional or taxon groups would increase the accuracy of scaling respiration to the plot level. All analyses were conducted using JMP (v. 8, SAS Institute).

Mean maintenance respiration per unit stem surface area (R_m) at each sample plot was estimated as the *y*-intercept of R_s plotted against growth rate, when growth rate is zero (Penning de Vries, 1975). Error was calculated as the *y*-intercept error from R_s regressed vs. growth rate. Growth respiration per unit stem area (R_g) was then calculated as the difference between total measured respiration and maintenance respiration; error was calculated from the sum of squares of R_s and R_m error estimates. The growth respiration coefficient, GRC, was calculated as the slope of the linear fit of R_s vs. growth rate, with error reported as the SE of the slope of R_s regressed against growth. Both maintenance and growth respiration were plotted against elevation for between-plot comparisons.

We also exploited the elevation gradient to estimate the sensitivity of stem respiration to temperature (assuming that temperature was the main driver (direct or indirect) of differences seen along the transect). We fit an exponential model to our data:

$$R_{\text{stem}} = R_{\text{stem}0} e^{-k(T-T_0)}, \quad (3)$$

where R_{stem} is the mean stem respiration at a point with

Table 2 Models used to predict tree heights in the Andean plots where (h) is predicted tree height and (d) is diameter at breast height

Plot	Elevation (m)	Height model	Model fit	Height correction factor
Tono	1000	$y = 6.06\ln(x) - 4.58$	0.79	0.86
San Pedro	1500	$y = 4.48\ln(x) - 1.48$	0.78	0.72
Wayqecha	3000	$y = 3.34\ln(x) + 0.49$	0.66	0.61

Plot-specific tree heights were incorporated into calculations of stem area index to account for changing tree allometries with elevation. Model fit is the r^2 value of the non-linear regression models. The height correction factor is used to correct for declining tree height with elevation relative to the Tambopata lowland sites (see text). Data from J. A. B. Fisher (unpublished analysis).

measured temperature T , and R_{stem0} is the reference respiration at an arbitrary reference temperature T_0 , and k is the temperature sensitivity coefficient.

In ecophysiological literature, this temperature sensitivity is often expressed as a Q_{10} coefficient, where Q_{10} is the change in respiration rate associated with a 10 °C change in temperature:

$$Q_{10} = e^{10k}, \quad (4)$$

where k is the slope of the regression of respiration against the natural logarithm of temperature (°C). The error in Q_{10} , ΔQ_{10} , can be calculated from the error in k , Δk , as:

$$\frac{\Delta Q_{10}}{Q_{10}} = 10\Delta k. \quad (5)$$

Our analyses describe apparent changes in ecosystem woody respiration that are not purely ecophysiological or metabolic (e.g. changes in active tissue depth, and changes in forest structure), and hence application of Q_{10} may be considered not strictly appropriate. Nevertheless, it is still conceptually useful to calculate a value of Q_{10} for comparative purposes (thus treating it as a general temperature sensitivity parameter) particularly in the context of ecosystem models that may incorporate a single Q_{10} response that includes both ecophysiological and structural responses to temperature.

Within each site, we tested for the best-fit relationship of R_s and growth rate and/or dbh for each tree. Models were set up to include both dbh and growth rate (with one model including an interaction term), and only dbh or growth rate. The Akaike Information Criterion (AIC) was used to select the best-fit model while penalizing models with more parameters (Kutner *et al.*, 2005). R_s was scaled up from the area under the chamber to the entire tree level, and then to the plot level ($R_{s \text{ plot}}$; $\text{Mg C ha}^{-1} \text{ yr}^{-1}$) by multiplying R_s by SAI using two methods. Method 1 takes the sum of $R_{s \text{ tree}} \times \text{SAI}_{\text{tree}}$ for each tree and then sums over all trees with $R_{s \text{ tree}}$ for each non-measured tree estimated from the site-specific diameter/growth rate model; method 2 is the product of the plot $R_{s \text{ mean}} \times \text{SAI}_{\text{plot}}$. As method 1 is a more rigorous approach than method 2, only the mean values from method 1 are reported herein; however, it is simpler to estimate propagated errors from method 2. Error values for $R_{s \text{ plot}}$ were calculated as the mean proportional sums of squares error of R_s and SAI_{plot} (error for $R_{m \text{ plot}}$ and $R_{g \text{ plot}}$ were calculated in the same manner). $\text{SAI}_{\text{total}}$ is the SAI_{plot} plus the estimated small-tree SAI. $R_{s \text{ total}}$ is the scaled R_s estimates to the 1-ha plot level also incorporated the estimated additional SAI of small trees <10 cm dbh. Even though the relationship between R_s per unit stem area and dbh was weak, total stem respiration is still likely to scale strongly with total stem surface area. $R_{g \text{ plot}}$ is calculated as the difference in $R_{s \text{ plot}}$ and $R_{m \text{ plot}}$.

Results

Measured woody respiratory flux

Plot mean stem CO_2 efflux per unit stem surface area varied over the elevation gradient approximately 1.7-

fold (Fig. 2, Table 3). There was also substantial variation among trees within sites, ranging between one and two orders of magnitude. An exponential regression of mean respiration rate per unit stem surface area at each site against mean annual temperature at that site resulted in a temperature sensitivity parameter, k , of $0.04 \pm 0.01 \text{ } ^\circ\text{C}^{-1}$ (adjusted $r^2 = 0.86$; $P = 0.016$), equivalent to a Q_{10} temperature sensitivity of 1.50 ± 0.12 .

In the 3025 m plot, there was no significant difference in measured woody carbon efflux per unit stem surface area between the dominant genus, *Weinmannia*, and other tree taxa in the plot ($t = 0.277$, $\text{df} = 47$, $P = 0.39$; mean R_s *Weinmannia* = $0.68 \pm 0.14 \mu\text{mol m}^{-2} \text{ s}^{-1}$, mean R_s all other genera = $0.54 \pm 0.05 \mu\text{mol m}^{-2} \text{ s}^{-1}$). There was a moderately significant difference in efflux per stem surface area values for palms as compared with broadleaf trees ($t = 1.36$, $\text{df} = 17$, $P = 0.096$; mean R_s palms = $1.13 \pm 0.24 \mu\text{mol m}^{-2} \text{ s}^{-1}$, mean R_s broadleaves = $0.75 \pm 0.12 \mu\text{mol m}^{-2} \text{ s}^{-1}$), but there was no significant difference in R_s between lianas and trees ($t = 1.76$, $\text{df} = 14$, $P = 0.45$; mean R_s lianas = $0.84 \pm 0.16 \mu\text{mol m}^{-2} \text{ s}^{-1}$, mean R_s trees = $1.01 \pm 0.28 \mu\text{mol m}^{-2} \text{ s}^{-1}$).

Maintenance and growth respiration

For each site, regressions of R_s vs. growth (Fig. 3) were used to calculate the GRC, maintenance and growth respiration for each plot. Maintenance respiration per unit stem surface area showed a moderately significant ($P < 0.10$) negative trend when regressed against elevation [adjusted $r^2 = 0.60$, $P = 0.08$, slope = $(-7.6 \pm 2.84) \times 10^{-3} \mu\text{mol m}^{-2} \text{ s}^{-1} \text{ m}^{-1}$ elevation; Fig. 4]. Growth respiration per unit stem area had a very similar absolute decline with elevation (adjusted $r^2 = 0.60$, $P = 0.07$, slope = $(-8.4 \pm 2.77) \times 10^{-5} \mu\text{mol C m}^{-2} \text{ s}^{-1} \text{ m}^{-1}$ elevation; Fig. 4), but a much greater proportional decline as mean growth respiration rates were much smaller. The growth respiration coefficient, GRC, showed a strong decline with elevation ($r^2 = 0.95$, $P = 0.004$, slope = $(-3.1 \pm 0.40) \times 10^{-4} \mu\text{mol m}^{-2} \text{ s}^{-1} \text{ cm}^{-1}$ growth m^{-1} elevation; Fig. 5). The GRC in particular appeared to decline to approximately zero at the highest elevation plot.

Extrapolation of R_s

To assign R_s to every tree within the 1-ha plots, the best-fit relationships characterizing stem CO_2 efflux per stem surface area given tree dbh and/or growth rate were used (Table 4). The model parameters for the TAM-05, 1000, and 3025 m plots were dbh and growth, while dbh alone best explained the trend of R_s vs. elevation in the TAM-06 and 1500 m plots.

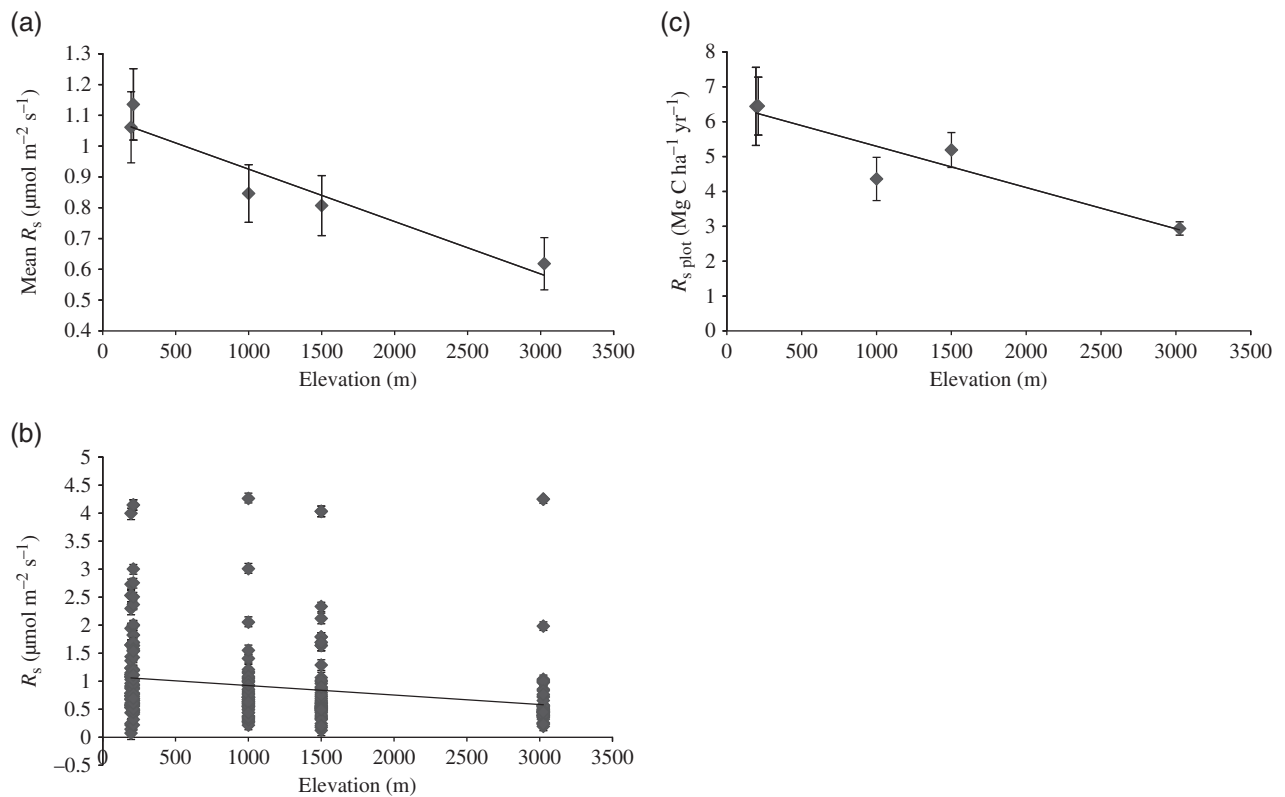


Fig. 2 Woody CO₂ efflux plotted against elevation. (a) Mean measured CO₂ efflux per unit stem surface area ($\mu\text{mol C m}^{-2} \text{s}^{-1}$; $r^2 = 0.92$, $P < 0.001$, slope = $(-1.7 \pm 0.30) \times 10^{-4} \mu\text{mol C m}^{-2} \text{sec}^{-1} \text{m}^{-1}$ elevation); $N = 44$ (194 m), 48 (210 m), 52 (1000 m), 48 (1500 m), 50 (3025 m). (b) All data points for measured trees in each 1-ha plot (CO₂ efflux per unit stem area) shown regressed against elevation (adjusted $r^2 = 0.06$, $P = 0.0001$, slope = $(-1.7 \pm 0.44) \times 10^{-4} \mu\text{mol C m}^{-2} \text{sec}^{-1} \text{m}^{-1}$ elevation); $N = 242$; (c) CO₂ efflux scaled to the 1-ha plot level ($\text{Mg C ha}^{-1} \text{yr}^{-1}$; adjusted $r^2 = 0.82$, $P = 0.02$, slope = $(-1.18 \pm 0.27) \times 10^{-3} \text{Mg C ha}^{-1} \text{yr}^{-1} \text{m}^{-1}$ elevation). Error bars indicate standard error of the mean.

Table 3 Measured respiration per stem surface area (R_s) from seven plots along an elevation gradient in the Peruvian Andes

Plot	Elevation (m)	N	R_s ($\mu\text{mol m}^{-2} \text{s}^{-1}$)	R_m ($\mu\text{mol m}^{-2} \text{s}^{-1}$)	R_g ($\mu\text{mol m}^{-2} \text{s}^{-1}$)	GRC ($\mu\text{mol m}^{-2} \text{s}^{-1} \text{cm}^{-1}$ growth)
TAM-06	194	44	1.06 ± 0.12	0.80 ± 0.14	0.26 ± 0.18	0.58 ± 0.21
TAM-06 _{small}	194	23	0.46 ± 0.04			
TAM-05	210	48	1.14 ± 0.12	0.86 ± 0.15	0.28 ± 0.19	0.73 ± 0.27
TAM-05 _{small}	210	27	0.96 ± 0.21			
Tono	1000	52	0.85 ± 0.09	0.66 ± 0.11	0.19 ± 0.14	0.51 ± 0.17
San Pedro	1500	48	0.81 ± 0.10	0.78 ± 0.11	0.03 ± 0.15	0.19 ± 0.40
Wayqecha	3025	50	0.62 ± 0.09	0.58 ± 0.11	0.03 ± 0.14	-0.2 ± 0.18

Small diameter trees (≤ 10 cm dbh) were measured in TAM-05_{small} and TAM-06_{small}, in all other plots trees and lianas ≥ 10 cm dbh were measured. R_m is the maintenance component; the growth component of stem respiration is R_g . GRC is the growth respiration coefficient.

Scaling R_s

SAI_{plot} showed no significant trend with elevation when the SAI equation was adjusted by plot-specific tree heights (Fig. 6; adjusted $r^2 = 0.08$, $P = 0.33$, slope = $(-8.5 \pm 7.37) \times 10^{-5} \text{m}^{-1}$ elevation). Without

the canopy-height adjustment, however, the SAI would have been overestimated in the Andean plots and thus would have generated a significant positive correlation between SAI and elevation (adjusted $r^2 = 0.60$, $P < 0.0001$, slope = $(3.05 \pm 1.15) \times 10^{-4} \text{m}^{-1}$ elevation). This illustrates the importance of including site-specific

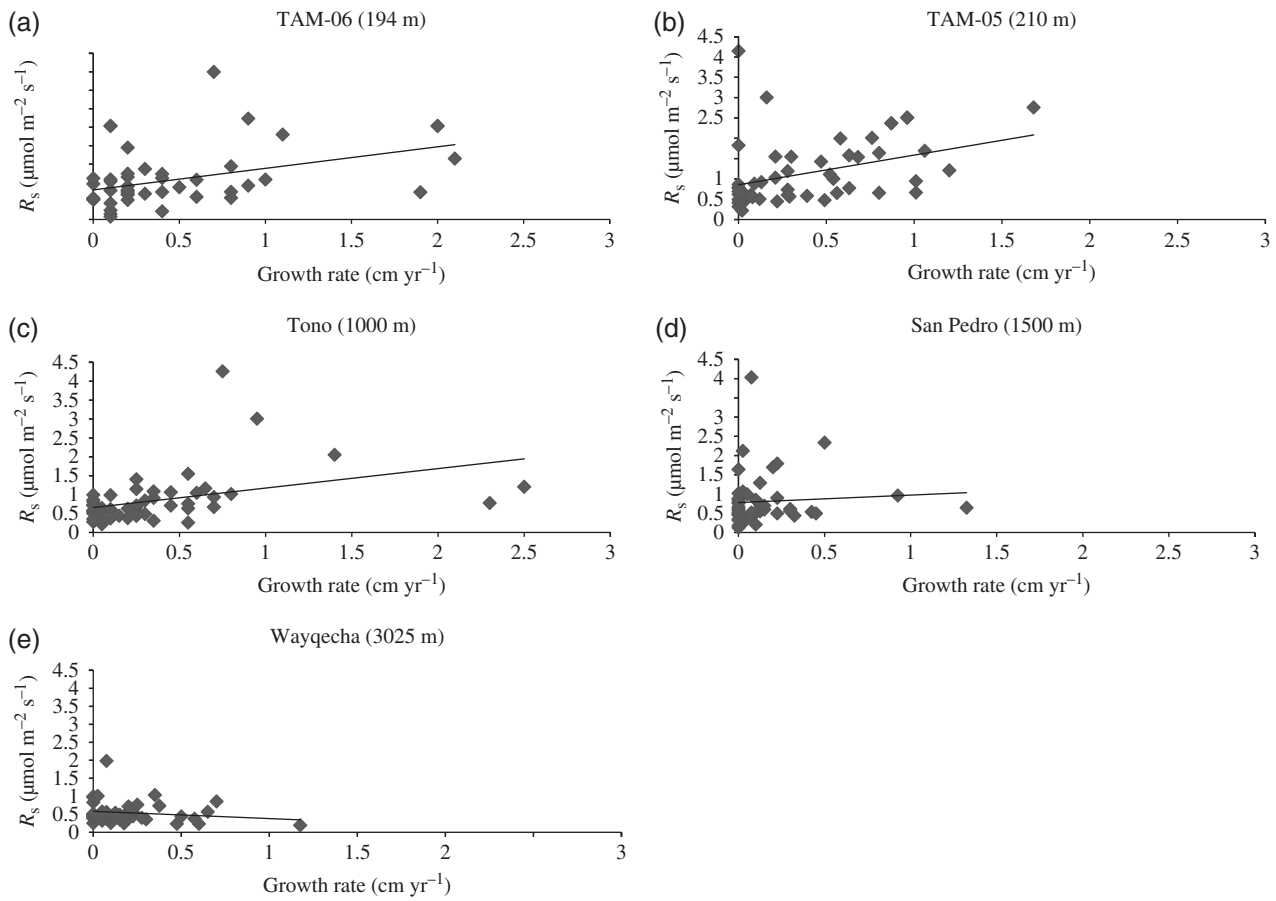


Fig. 3 Measured CO₂ efflux per unit stem surface area ($\mu\text{mol C m}^{-2} \text{s}^{-1}$) regressed against growth rate for each 1-ha plot. Each point represents an individual tree. TAM06 (194 m) adjusted $r^2 = 0.14$, $P < 0.01$, slope = 0.58 ± 0.21 ; TAM05 (210 m) adjusted $r^2 = 0.11$, $P = 0.01$, slope = 0.73 ± 0.27 ; Tono (1000 m) adjusted $r^2 = 0.13$, $P = 0.01$, slope = 0.51 ± 0.17 ; San Pedro (1500 m) adjusted $r^2 = 0.01$, $P = 0.63$, slope = 0.19 ± 0.40 ; Wayqecha (3025 m) adjusted $r^2 = 0.03$, $p = 0.28$, slope = -0.20 ± 0.18 .

tree allometries whenever possible when using this method, in particular along environmental gradients where tree form is likely to change. The relative constancy of SAI (with the allometric adjustment) is the net result of two compensating trends in forest structure. The decline in tree stature with increasing elevation tends to decrease overall stem surface area, but this effect is offset by the increasing number of small trees, which tends to increase overall stem surface area.

Consideration of small trees < 10 cm dbh substantially increased the estimated SAI of the plot, by $0.19 \text{ m}^2 \text{ m}^{-2}$ (13%) at 3250 m, by $0.30 \text{ m}^2 \text{ m}^{-2}$ (15%) at 1500 m, and by $0.16\text{--}0.24 \text{ m}^2 \text{ m}^{-2}$ (9–14%) at the lowland sites (ca. 200 m). Averaging the percentage small tree SAI contribution at 194, 210 and 1500 m, we estimate that the small tree SAI at 1000 m would be $0.23 \pm 0.02 \text{ m}^2 \text{ m}^{-2}$ (9%).

The results of scaling stem respiration to the plot level, in $\text{Mg C ha}^{-1} \text{ yr}^{-1}$ are shown in Table 5. Scaled CO₂ efflux ha^{-1} values were calculated with SAI esti-

mates that were adjusted for the reduction in canopy height with increasing elevation. As R_s was not measured in the small diameter plots in the montane sites, the additional SAI of the small trees for 1500 and 3025 m was accounted for by multiplying the calculated $R_{s \text{ plot}}$ by $\text{SAI}_{\text{total}}/\text{SAI}_{\text{plot}}$. This correction increased estimates of $R_{s \text{ total}}$ by between 9% (1000 m) and 15% (1500 m). Including small trees when estimating overall SAI is clearly important in scaling respiration to the plot level.

Keeping with the assumption that all variation in woody CO₂ efflux along the transect is primarily determined by temperature (an assumption unlikely to be entirely true as the transect spans gradients such as changes in tree species composition, moisture, and soil types), we can also quantify a temperature sensitivity of ecosystem-level stem carbon efflux, incorporating the variation of physiological respiration rate and the variation of stem area index. An exponential regression of stem CO₂ efflux per unit ground area, $R_{s \text{ total}}$, against mean annual temperature at that site resulted in

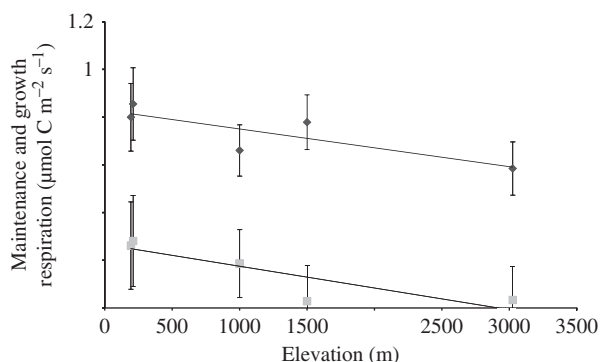


Fig. 4 Estimated maintenance respiration per unit stem surface area and growth respiration per unit stem surface area for woody tissues for each plot. Dark grey diamonds represent values for maintenance stem respiration; the line shows trend of maintenance respiration (R_m) with elevation (adjusted $r^2 = 0.60$, $P = 0.08$, slope = $(-7.6 \pm 2.84) \times 10^{-3} \mu\text{mol C m}^{-2} \text{sec}^{-1} \text{m}^{-1}$ elevation). Light grey squares show growth stem respiration (R_g); line shows trend with elevation (adjusted $r^2 = 0.67$, $P = 0.06$ slope = $(-8.4 \pm 2.77) \times 10^{-5} \mu\text{mol C m}^{-2} \text{s}^{-1} \text{m}^{-1}$ elevation). Error bars are the standard error of the mean; lower bars are removed for the upper two elevations as they were below zero.

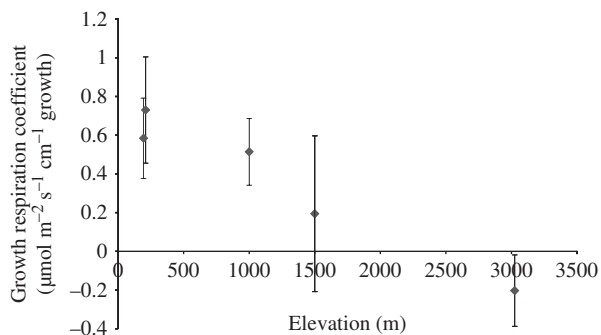


Fig. 5 Growth rate coefficient (GRC; $\mu\text{mol m}^{-2} \text{s}^{-1} \text{cm}^{-1}$ growth) for each plot in the elevation transect (adjusted $r^2 = 0.95$, $P < 0.01$, slope = $(-3.1 \pm 0.40) \times 10^{-4} \mu\text{mol m}^{-2} \text{s}^{-1} \text{cm}^{-1} \text{growth m}^{-1}$ elevation GRC was calculated as the slope of the regression of stem CO_2 efflux against growth rate).

a temperature sensitivity parameter, k , of $0.048 \pm 0.012 \text{ } ^\circ\text{C}^{-1}$ (adjusted $r^2 = 0.96$; $P < 0.01$), equivalent to a Q_{10} temperature sensitivity of 1.62 ± 0.19 , similar to the value of $Q_{10} = 1.51 \pm 0.04$ when only respiration rates per unit stem area are considered. The Q_{10} value of maintenance respiration are similar ($Q_{10} = 1.42 \pm 0.25$ at plot level, $Q_{10} = 1.27 \pm 0.10$ at stem level); the value for growth respiration is much greater but with large uncertainty ($Q_{10} = 5.83 \pm 2.97$ at plot level, $Q_{10} = 5.63 \pm 3.09$ at stem level). Hence plot mean maintenance and overall stem respiration rates appear to have relatively low sensitivity to temperature, whether on a stem surface area basis or a plot area basis.

Discussion

There is a clear trend of decreasing stem CO_2 efflux with increasing elevation, even given the high within-plot variation. We did not see the six-fold decline in R_s found across a 2000-m elevation transect in the Ecuadorian Andes (Zach *et al.*, 2010). R_s follows the pattern of declining above-ground and below-ground net primary productivity (NPP) with elevation (Girardin *et al.*, in press), with a similar range of variation along the elevation transect. In comparison, respiration per unit mass of soil organic matter does show a strong decline along the transect (Zimmermann *et al.*, 2009), as does leaf litter decay (Salinas *et al.*, in press). Autotrophic processes appear to vary less along the gradient than heterotrophic processes; in the long-term, autotrophic respiration has to be limited by photosynthetic substrate supply. This difference in temperature sensitivity between autotrophic production processes and heterotrophic decomposition processes explains the accumulation of the litter layer and soil organic matter in cold ecosystems, such as at the top of this transect.

Our data suggest that the variation in R_s with increasing elevation is driven by changes in both maintenance and growth respiration. The relatively little variation of maintenance respiration is remarkable in the context of the large variation in temperature and the complete turnover of tree community composition along the gradient.

The decline of growth respiration with elevation tracks the decline in growth rates, but the parallel apparent decline in the growth respiration coefficient is puzzling. Similarly, the apparent negative values of GRC at the highest elevation are impossible. At face value, this would imply that the construction cost of new woody tissue declines with elevation (or decreasing temperature) to effectively zero at the highest plot. One possible explanation for these paradoxes may be that our assumption of a simple mean maintenance respiration rate applicable to all trees and functional groups in a plot is invalid. If faster growing trees have lower maintenance respiration rates than slow-growing trees at the high-elevation plots, this would generate an apparent decline in GRC and a slight increase in the intercept (estimated maintenance respiration). This would imply that our overall maintenance respiration rates were overestimated at the high elevation plots. Ryan *et al.* (2009) showed that both maintenance respiration and growth respiration coefficients declined with tree age, as does tree growth rate. This does not easily explain the trend in GRC with elevation, however, as trees are no older at the high elevation plots (tree turnover times are similar along the elevation transect).

Table 4 Model parameters for assigning R_s values to each tree in 1-ha plots based on subset of measured trees

Plot	Predictor var.	Model	Model fit
TAM-05	dbh and growth rate	$y = \exp^{(m \times -1/\sqrt{x}1 + m2 \times \sqrt{x}2 + b)}$	0.27
TAM-06	dbh	$y = \exp^{(m \times -1/\sqrt{x} + b)}$	0.21
TAM-05 _{small}	Growth rate	$y = \exp^{(m \times \sqrt{x} + b)}$	0.01
TAM-06 _{small}	Growth rate	$y = \exp^{(m \times \sqrt{x} + b)}$	0.01
Tono	dbh and growth rate	$y = \exp^{(m \times -1/\sqrt{x}1 + m2 \times \sqrt{x}2 + b)}$	0.40
San Pedro	dbh	$y = \exp^{(m \times -1/\sqrt{x} + b)}$	0.07
Wayqecha	dbh and growth rate	$y = \exp^{(m \times -1/\sqrt{x}1 + m2 \times \sqrt{x}2 + b)}$	0.12

Akaike Information Criterion was used to choose the best-fit model per site. m is the slope of the regression, x is the independent variable and b is the y -intercept. Model fit is the r^2 coefficient of determination for the model.

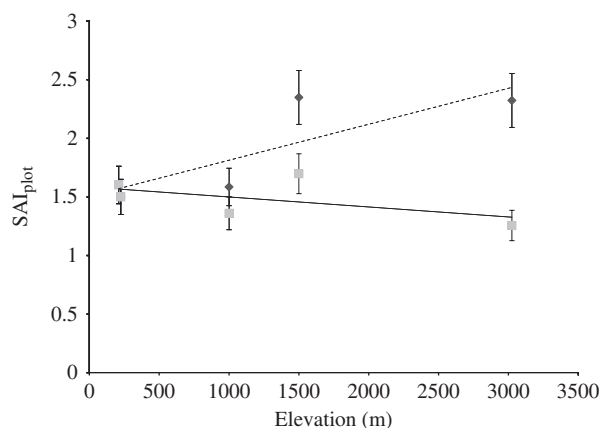


Fig. 6 Stem Area Index per 1-ha plot (SAI_{plot} ; m^2 stem surface area m^{-2} ground) regressed against elevation. Diamonds represent plot SAI_{plot} before adjustment for plot-specific canopy height (dashed line; adjusted $r^2 = 0.60$, $P = 0.08$, [slope = $(3.05 \pm 1.15) \times 10^{-4}$]; squares represent SAI_{plot} after canopy height adjustment [solid line; adjusted $r^2 = 0.08$, $P = 0.33$, slope = $(-8.5 \pm 7.4) \times 10^{-5}$]. The inclusion of differences in stem allometry along the transect has a strong influence on estimates of SAI and thus of total stem respiration. SAI error is assigned to be 10% (see text).

Our measurements present only a snapshot from the early dry season, yet data on the seasonal variation in stem growth rates provides some indication that our inferences about annual stem respiration rates are robust. C. A. J. Girardin, Y. Malhi, L. Durand, L. E. O. C. Araújo, R. J. Whittaker, M. Zimmermann, J. E. Silva-Espejo, N. Salinas (unpublished results) report on seasonal variation in tree growth rates across these sites. They report almost no seasonality in tree growth rates at the 1000 and 3025 m sites and only moderate seasonality in growth at the 194, 210, and 1500 m sites, with peak growth in the wet season (January–February) and minimum growth in the dry season (June–September). Our sample period of May falls between these extremes and represents a period when growth rates are likely to be

representative of the annual mean growth rates. Zach *et al.* (2010) found stem respiration to be highest during the driest months in a tropical montane forest. Detailed seasonal comparisons of stem respiration have recently commenced at a number of plots along this transect, and will eventually enable evaluation of the magnitude of seasonal variation.

Unexpectedly, we found no significant relationship (at 5%) between stem CO_2 efflux and forest functional types, although this analysis is limited by the small sample sizes of each functional type. There is a hint that palms have higher respiration rates than broadleaf trees ($P < 0.10$), and this difference may have become more significant with larger sample sizes. Functional and genus-specific differences in R_s have been documented in Central-American forests (Cavaleri *et al.*, 2006, 2008), although variation at the genus level at that site is likely due to the nitrogen-fixing habit of the dominant genus, *Pentaclethra*. Maintenance respiration is expected to vary with tissue N content (Ryan, 1991; Reich *et al.*, 2008).

The difference in plot-level R_s with and without the incorporation of small trees and lianas between 2 and 10 cm dbh, shows the important contribution of small trees to ecosystem respiration (R_{eco}). Small-tree carbon efflux per ha increased plot R_s estimates by 9–15%, a component that is not generally included in plot-level analyses. Moreover, as the understory may show substantial site-to-site variation, using site-specific SAI values where possible is important. Cavaleri *et al.* (2008) found higher respiration rates from branches than in the trunk. Small diameter branches were not included in our measurements (although large branches are incorporated into the SAI equation; Chambers *et al.*, 2004). This suggests that our values reported here may be underestimated (see Malhi *et al.*, 2009), although it is unclear how much of the CO_2 efflux from branches represents plant stem metabolism as opposed to the release of soil CO_2 efflux dissolved in the transpiration stream.

We used Q_{10} to demonstrate the relationship of CO_2 efflux from woody tissues with temperature along our

Table 5 Stem area index per plot (SAI_{plot}) and stem respiration ($R_{s, plot}$) scaled to 1-ha plot level

Plot	Elevation (m)	N	SAI_{plot}	SAI_{plot} canopy-height corrected	SAI_{total}	$R_{s, plot}$ ($Mg\ C\ ha^{-1}\ yr^{-1}$)	$R_{s, total}$ ($Mg\ C\ ha^{-1}\ yr^{-1}$)	$R_{m, plot}$ ($Mg\ C\ ha^{-1}\ yr^{-1}$)	$R_{g, plot}$ ($Mg\ C\ ha^{-1}\ yr^{-1}$)
TAM-06	194	667	1.60 ± 0.16	1.60 ± 0.16	1.76 ± 0.18	6.44 ± 1.12	6.71 ± 1.12	5.20 ± 0.51	1.24 ± 0.21
TAM-06 _{small}	194	89		0.16 ± 0.02		0.27 ± 0.06			
TAM-05	210	539	1.50 ± 0.15	1.50 ± 0.15	1.74 ± 0.17	6.45 ± 0.83	7.31 ± 0.83	4.55 ± 0.51	1.90 ± 0.22
TAM-05 _{small}	210	88		0.24 ± 0.02		0.86 ± 0.02			
Tono	1000	447	1.59 ± 0.16	1.36 ± 0.14	1.59 ± 0.16	4.36 ± 0.62	5.09 ± 1.27	3.40 ± 0.25	0.96 ± 0.12
San Pedro	1500	887	2.35 ± 0.24	1.70 ± 0.17	2.00 ± 0.20	5.19 ± 0.50	6.08 ± 0.50	5.01 ± 0.32	0.18 ± 0.15
1500 _{small}	1500	72		0.30 ± 0.03					
Wayqecha	3025	1151	2.32 ± 0.23	1.26 ± 0.13	1.45 ± 0.15	2.94 ± 0.19	3.38 ± 0.28	2.78 ± 0.19	0.16 ± 0.14
3025 _{small}	3025	175		0.19 ± 0.02					

SAI_{total} is SAI_{plot} plus the SAI from estimated understorey component (small-diameter tree plots). Height-corrected SAI values incorporate the decreasing canopy height with elevation. $R_{s, total}$ includes the estimated contribution of understorey stem respiration. $R_{m, plot}$ and $R_{g, plot}$ are maintenance and growth respiration, respectively, scaled to the 1-ha plot for all trees > 10 cm dbh (i.e. $R_{s, plot} = R_{m, plot} + R_{g, plot}$). N is the total number of trees and lianas ≥ 10 cm dbh in each plot, with exception of the small-diameter plots which only included trees and lianas 2 \geq dbh ≤ 10 . The understorey SAI for the Tono (1000 m) plot was estimated by using the average of 1500_{small}, TAM-05_{small}, and TAM-06_{small} to calculate SAI_{total} .

elevation transect. In doing so, we assume that temperature is the unique variable differing across the elevation gradient. Clearly, this assumption is not fully met, as other variables such as soil nutrients and species composition and structure also vary between these plots.

We did not take into account diurnal variations in R_s which may cause our estimates to be overestimated if stem CO_2 efflux rates decline at night. R_s rates measured in a montane tropical forest in Ecuador did not significantly differ over a 24-hour period (Zach *et al.*, 2008), but variability in diurnal xylem sap flow rates can cause variation in bole CO_2 efflux (Teskey & McGuire, 2002). As our measurements are all taken during the day when xylem flow rates are high, there is less CO_2 diffusing through the bark from the xylem (Teskey & McGuire, 2002). Nevertheless, we did not attempt to separate the sources of C efflux between xylem-transported and local tissue metabolites. How xylem-transported C varies with elevation is unknown.

Conclusions

The data presented here show that there is a substantial (two-fold) variation in stem CO_2 efflux with elevation in our Amazon-Andes transect. This variation is driven by an apparent decline in both maintenance and growth respiration. At plot level, the rate of decline is very sensitive to changes in forest structure, but in this case the decline in tree stature was offset by the increase in small trees, leading to little overall change in stem surface area. The moderate sensitivity to elevation, and implicitly to temperature, suggests that autotrophic processes have moderate long-term sensitivity to temperature, in contrast to heterotrophic processes.

The bottom-up approach of providing detailed quantification of carbon cycling at the plot level generates new insights into the carbon budget of tropical ecosystems (Malhi *et al.*, 2009). The results presented here add to a growing pool of information on autotrophic respiration in tropical forests, although it remains among the least studied aspect of forest carbon dynamics.

We can speculate on how global warming trends will affect woody-tissue respiration rates in the tropics. The tropical Andes are predicted to warm by 4–6 °C this century under mid-high greenhouse gas emissions scenarios (Urrutia & Vuille, 2009). Our data suggest that plot-level stem respiration rates are likely to increase with warming, but that this increase would be sensitive to (i) changes in forest stature and woody surface area, (ii) increases in forest growth rates (either because of the physiology of growth or enhanced nutrient supply because of more rapid mineralization rates – which are likely to change faster than autotrophic metabolic processes), and (iii) increases in long-term maintenance

respiration rates. Our findings are based on sites in a quasi-equilibrium with mean annual temperatures; systems experiencing a rapid 4–6 °C warming over a century are likely to display a number of transient phenomena as physiological and ecological processes respond to such rapid changes in abiotic factors. We have demonstrated the power of elevation transects to reveal insights into how complex systems adjust in both structure and physiology to changes in mean annual temperature. Tropical elevation transects may prove particularly powerful tools as they avoid the confounding interactions with variability of growing season and seasonal variation in temperature and soil moisture that may be found in mid-high latitude elevation transects. Such insights need to be explored further in continued and more detailed measurements at this elevation transect, and parallel studies in other elevation transects across the tropics.

Acknowledgements

This study is a product of the Andes Biodiversity and Ecosystems Research Group ABERG, <http://darwin.winston.wfu/andes>. It was financed by grants from the Natural Environment Research Council (NE/D014174/1), and from the Gordon and Betty Moore Foundation. Yadvinder Malhi is supported by the Jackson Foundation. We would like to thank the Asociacion para la Conservacion de la Cuenca Amazonica (ACCA) for the use of the Wayqecha field station, and Explorers Inn for the use of Tambopata field station. Also, we thank Norma Salinas for assistance in obtaining INRENA permits to work within the Manu National Park. Becky Morris prepared Fig. 1.

References

- Aragão LEOC, Malhi Y, Metcalfe DB *et al.* (2009) Above- and below-ground net primary productivity across ten Amazonian forests on contrasting soils. *Biogeosciences*, **6**, 2759–2778.
- Aubrey DP, Teskey RO. (2009) Root-derived CO₂ efflux via xylem stream rivals soil CO₂ efflux. *New Phytologist*, **184**, 35–40.
- Bowman WP, Barbour MM, Turnbull MH, Tissue DT, Whitehead D, Griffin KL (2005) Sap flow rates and sapwood density are critical factors in within- and between-tree variation in CO₂ efflux from stems of mature *Dacrydium cupressinum* trees. *New Phytologist*, **167**, 815–828.
- Cavaleri MA., Oberbauer SF., Ryan MG. (2006) Wood CO₂ efflux in a primary tropical rain forest. *Global Change Biology*, **12**, 2442–2458.
- Cavaleri MA., Oberbauer SF., Ryan MG. (2008) Foliar and ecosystem respiration in an old-growth tropical rain forest. *Plant, Cell and Environment*, **31**, 473–483.
- Chambers JQ, dos Santos J, Ribeiro RJ, Higuchi N (2009) LBA-ECO CD-08 Tree inventory data, Ducke Reserve, Manaus, Brazil: 1999. Data set. Available at: <http://daac.ornl.gov> from Oak Ridge National Laboratory Distributed Active Archive Center, Oak Ridge, TN, USA. doi: 10.3334/ORNDAAC/910.
- Chambers JQ, Tribuzy ES, Toledo LC *et al.* (2004) Respiration from a tropical forest ecosystem: partitioning of sources and low carbon use efficiency. *Ecological Applications*, **14**, 72–78.
- Frangi JL, Lugo AE (1985) Ecosystem dynamics of a subtropical floodplain forest. *Ecological Monographs*, **55**, 351–369.
- Girardin CAJ, Malhi Y, Aragão LEOC *et al.* (2010) Net primary productivity allocation and cycling of carbon along a tropical forest elevation transect in the Peruvian Andes. *Global Change Biology*, **16**, 3176–3192.
- Hansen LD, Hopkin MS, Rank DR, Anekonda TS, Breidenbach RW, Criddle RS (1994) The relation between plant growth and respiration: a thermodynamic model. *Planta*, **194**, 77–85.
- Harris NL, Hall CAS, Lugo AE (2008) Estimates of species- and ecosystem-level respiration of woody stems along an elevational gradient in the Luquillo Mountains, Puerto Rico. *Ecological Modelling*, **216**, 253–264.
- Kutner MH, Nachtsheim CJ, Neter J, Li W (2005) *Applied Linear Statistical Models*, 5 edn. McGraw-Hill Irwin, New York, pp. 353–360.
- Luyssaert S, Inglima I, Jung M *et al.* (2007) CO₂ balance of boreal, temperate, and tropical forests derived from a global database. *Global Change Biology*, **13**, 2509–2537.
- Malhi Y, Aragão LEOC, Metcalfe DB *et al.* (2009) Comprehensive assessment of carbon productivity, allocation and storage in three Amazonian forests. *Global Change Biology*, **15**, 1255–1274.
- Malhi Y, Baker TR, Phillips OL *et al.* (2004) The above-ground coarse-wood productivity of 104 Neotropical forest plots. *Global Change Biology*, **10**, 563–591.
- Malhi Y, Grace J (2000) Tropical forests and atmospheric carbon dioxide. *Trends in Ecology and Evolution*, **15**, 332–337.
- Meir P, Metcalfe DB, Costa ACL, Fisher RA (2008) The fate of assimilated carbon during drought: impacts on respiration in Amazon rainforests. *Philosophical Transactions of the Royal Society*, **363**, 1849–1855.
- Meir P, Grace J (2002) Scaling relationships for woody tissue respiration in two tropical rainforests. *Plant, Cell and Environment*, **25**, 963–973.
- Penning de Vries FWT (1975) The cost of maintenance processes in plant cells. *Annals of Botany*, **39**, 77–92.
- Phillips OL, Aragão LEOC, Lewis SL *et al.* (2009) Drought sensitivity of the Amazon rainforest. *Science*, **323**, 1344–1347.
- Reich PB, Tjoelker MG, Pregitzer KS, Wright IJ, Oleksyn J, Machado JL (2008) Scaling of respiration to nitrogen in leaves, stems and roots of higher land plants. *Ecology Letters*, **11**, 793–801.
- Ryan MG (1990) Growth and maintenance respiration in stems of *Pinus contorta* and *Picea engelmannii*. *Canadian Journal of Forestry Research*, **20**, 48–57.
- Ryan MG (1991) Effects of climate change on plant respiration. *Ecological Applications*, **1**, 157–167.
- Ryan MG, Cavaleri MA, Almeida AC, Penchel R, Senock RS, Stape JL (2009) Wood CO₂ efflux and foliar respiration for *Eucalyptus* in Hawaii and Brazil. *Tree Physiology*, **29**, 1213–1222.
- Ryan MG, Gower ST, Hubbard RM, Waring RH, Gholz HL, Cropper WP, Running SW (1995) Woody tissue maintenance respiration of four conifers in contrasting climates. *Oecologia*, **101**, 133–140.
- Salinas N, Malhi Y, Meir P *et al.* (in press) The sensitivity of leaf litter decomposition to temperature: results from a large-scale leaf translocation experiment along an elevation gradient in tropical Andean forests. *New Phytologist*.
- Saxe H, Cannell MGR, Johnsen O, Ryan MG, Vourlitis G (2001) Tansley review no. 123: tree and forest functioning in response to global warming. *New Phytologist*, **149**, 369–400.
- Teskey RO, McGuire MA (2002) Carbon dioxide transport in xylem causes errors in estimation of rates of respiration in stems and branches of trees. *Plant, Cell & Environment*, **25**, 1571–1577.
- Trumbore S (2006) Carbon respired by terrestrial ecosystems – recent progress and challenges. *Global Change Biology*, **12**, 141–153.
- Urrutia R, Vuille M (2009) Climate change projections for the tropical Andes using a regional climate model: temperature and precipitation simulations for the end of the 21st century. *Journal Geophysical Research*, **114**, D02108, doi: 10.1029/2008JD011021.
- Zach A, Horna V, Leuschner C (2008) Elevational change in woody tissue CO₂ efflux in a tropical mountain rain forest in southern Ecuador. *Tree Physiology*, **28**, 67–74.
- Zach A, Horna V, Leuschner C, Zimmerman R (2010) Patterns of wood carbon dioxide efflux across a 2,000-m elevation transect in an Andean moist forest. *Oecologia*, **162**, 127–137.
- Zimmermann M, Meir P, Bird MI, Malhi Y, Ccahuana AJQ (2009) Climate dependence of heterotrophic soil respiration from a soil-translocation experiment along a 3000 m tropical forest altitudinal gradient. *European Journal of Soil Science*, **60**, 895–906.